Cerebral Cortex January 2014;24:67–80
doi:10.1093/cercor/bhs284
Advance Access publication September 20, 2012

Homeostatic Control of Synaptic Activity by Endogenous Adenosine is Mediated by Adenosine Kinase

Maria José Diógenes[1,2], Raquel Neves-Tomé[1,2], Sergio Fucile[3,4], Katiuscia Martinello[4], Maria Scianni[3], Panos Theofilas[6], Jan Lopatář[5], Joaquim A. Ribeiro[1,2], Laura Maggi[3], Bruno G. Frenguelli[5], Cristina Limatola[3,4], Detlev Boison[6], and Ana M. Sebastião[1,2]

[1]Institute of Pharmacology and Neurosciences, Faculty of Medicine and [2]Unit of Neurosciences, Institute of Molecular Medicine, University of Lisbon, Lisbon, Portugal [3]Department of Physiology and Pharmacology, Institute Pasteur-Cenci Bolognetti Foundation, University Sapienza, Rome, Italy [4]IRCCS Neuromed, Pozzilli, Italy [5]School of Life Sciences, University of Warwick, Coventry CV4 7AL, UK and [6]R.S. Dow Neurobiology Laboratories, Legacy Research Institute, Portland, OR 97232, USA

Address correspondence to Maria José Diógenes, Institute of Pharmacology and Neurosciences, Faculty of Medicine and Unit of Neurosciences, Institute of Molecular Medicine, University of Lisbon, Av. Professor Egas Moniz, Lisbon 1649-028, Portugal. Email: diogenes@fm.ul.pt

M.J.D., R.N.-T., and S.F. have contributed equally to this work as 1st authors.
D.B. and A.M.S. have contributed equally to this work as senior authors.

Extracellular adenosine, a key regulator of neuronal excitability, is metabolized by astrocyte-based enzyme adenosine kinase (ADK). We hypothesized that ADK might be an upstream regulator of adenosine-based homeostatic brain functions by simultaneously affecting several downstream pathways. We therefore studied the relationship between ADK expression, levels of extracellular adenosine, synaptic transmission, intrinsic excitability, and brain-derived neurotrophic factor (BDNF)-dependent synaptic actions in transgenic mice underexpressing or overexpressing ADK. We demonstrate that ADK: 1) Critically influences the basal tone of adenosine, evaluated by microelectrode adenosine biosensors, and its release following stimulation; 2) determines the degree of tonic adenosine-dependent synaptic inhibition, which correlates with differential plasticity at hippocampal synapses with low release probability; 3) modulates the age-dependent effects of BDNF on hippocampal synaptic transmission, an action dependent upon co-activation of adenosine A_{2A} receptors; and 4) influences $GABA_A$ receptor-mediated currents in CA3 pyramidal neurons. We conclude that ADK provides important upstream regulation of adenosine-based homeostatic function of the brain and that this mechanism is necessary and permissive to synaptic actions of adenosine acting on multiple pathways. These mechanistic studies support previous therapeutic studies and implicate ADK as a promising therapeutic target for upstream control of multiple neuronal signaling pathways crucial for a variety of neurological disorders.

Keywords: adenosine, brain-derived neurotrophic factor, GABA, homeostasis, transgenic mice

Introduction

Despite intense drug development efforts during the past 40 years, the treatment of neurological conditions remains problematic and largely restricted to symptom control. The "holy grail" of pharmaceutical drug development is specificity and selectivity for identifiable downstream pathways of complex biological networks. The pharmacological blockade of selected pathways might be suitable for symptom control, but is unlikely to affect complex pathogenic processes in neurology that involve entire molecular, biochemical, and physiological networks.

In this regard, normal brain function depends on tightly controlled network homeostasis that is coupled to brain bioenergetics and metabolism. The modulation of adenosine signaling, a key link between brain bioenergetics and neuronal and astrocytic network homeostasis, is considered a rational therapeutic approach to treat neurological conditions on a network level in conditions ranging from epilepsy to schizophrenia (Wilz et al. 2008; Boison and Stewart 2009; Boison et al. 2011; Boison et al. 2012). The net effect of adenosine in most brain areas is the inhibition of neuronal activity mediated by adenosine A_1 receptors (A_1R), the predominant adenosine receptor subtype in the hippocampus. The potent antiepileptic activity of adenosine depends largely on the availability of A_1Rs (Dunwiddie 1980), though other adenosine receptors may also play a role (Etherington and Frenguelli 2004; Roseti et al. 2008, 2009; Sebastião and Ribeiro 2009; Sebastião 2010).

Adenosine A_{2A} receptors ($A_{2A}R$) in the hippocampus are largely devoted to regulating the activity of other neuromodulators (Sebastião and Ribeiro 2009). For example, $A_{2A}R$ activation gates the synaptic actions of brain-derived neurotrophic factor (BDNF), which are fully lost upon $A_{2A}R$ blockade (Diógenes et al. 2004, 2007, 2011; Pousinha et al. 2006; Fernandes et al. 2008; Fontinha et al. 2008; Tebano et al. 2008; Assaife-Lopes et al. 2010) or genetic deletion of $A_{2A}R$ (Tebano et al. 2008).

Adenosine kinase (ADK), by phosphorylating intracellular adenosine to AMP, maintains an inward adenosine gradient, driving adenosine influx into the cell (Boison et al. 2010). When ADK levels are pathologically or experimentally increased, the resulting adenosine deficiency directly translates into increased susceptibility to seizures or neuronal injury (Pignataro et al. 2007; Li, Ren et al. 2008). Conversely, a decrease in ADK activity leads to increased extracellular adenosine concentration (Etherington et al. 2009) and resistance to epileptic seizures or neuronal cell loss (Li, Lan et al. 2008; Li, Ren et al. 2008; Shen et al. 2011).

We hypothesized that ADK, as the primary determinant of adenosine levels, could act as a homeostatic bioenergetic network regulator, providing synergistic control of several downstream pathways simultaneously. We focused on ADK as a potential upstream regulator of BDNF-, glutamate-, and GABA-dependent synaptic signaling in the hippocampus. To test our hypothesis, we used transgenic mice that underexpress (Fb-Adk-def) or overexpress ADK (Adk-tg) in the forebrain.

Our data characterize ADK as an upstream regulator of multiple signaling pathways that depend on 1) $A_{2A}R$ via BDNF-mediated synaptic actions, 2) A_1R via the modulation of synaptic transmission and short-term plasticity, or 3) a combined action upon different adenosine receptor subtypes, via the modulation of $GABA_A$ current stability, and therefore suggest that ADK might be a prime therapeutic target to modulate networks synergistically.

Materials and Methods

Animals and Tissue Preparation

Three different genotypes of mice were used in this study, all maintained on an identical C57BL/6 background: 1) Wild-type (WT); 2) homozygous Adk-tg mice with brain-wide overexpression of a constitutively expressed loxP-flanked ADK transgene, but lack of the endogenous dynamically expressed *Adk* gene; these animals are characterized by a global overexpression of ADK throughout the hippocampal formation and have been described previously (Fedele et al. 2005; Pignataro et al. 2007; Yee et al. 2007; Li, Lan et al. 2008; Li, Ren et al. 2008); 3) Fb-Adk-def mice with reduced levels of forebrain ADK were created based on Emx1-Cre-driven deletion of the loxP-flanked *A*DK transgene in Adk-tg mice (Li, Ren et al. 2008). Adk-tg and Fb-Adk-def mice were derived as littermates according to our previous studies (Li, Ren et al. 2008; Masino et al. 2012) and controls were age- and sex-matched based on parallel breeding of C57BL/6 WT mice. All animals were genotyped at weaning as described previously (Fedele et al. 2005). Most experiments were performed in adult (>7 weeks old) animals. Since the effects of BDNF are age-dependent (Diógenes et al. 2007, 2011), 2 clearly distinct groups of animals were used: 3–5 weeks old (young) and 10–12 weeks old (adult).

All experimental procedures were performed in accordance with European Union guidelines and UK, Portuguese, or Italian regulations for the use of laboratory animals. Animals were either deeply anesthetized with halothane before killing by decapitation or killed by cervical dislocation. The brain was then quickly removed and either immersed in ice-cold gassed (95% O_2 and 5% CO_2, pH 7.4) artificial cerebrospinal fluid (aCSF) for subsequent cutting of parasagittal sections, or the hippocampus was dissected free in ice-cold aCSF. In both cases, the aCSF comprised: NaCl 124 mM, KCl 3 mM, NaH_2PO4 1.25 mM, $NaHCO_3$ 26 mM, $MgSO_4$ 1 mM, $CaCl_2$ 2 mM, and glucose 10 mM. When preparing slices for whole-cell recordings, a glycerol-based aCSF was used (glycerol 250 mM, KCl 2.5 mM, $CaCl_2$ 2.4 mM, $MgCl_2$ 1.2 mM, NaH_2PO_4 1.2 mM, $NaHCO_3$ 26 mM, glucose 11 mM, and Na-pyruvate 0.1 mM, pH 7.35), to better preserve neurons from Na^+-induced excitotoxicity. Slices (350–400 μm thick for field excitatory postsynaptic potential [fEPSP] and sensor recordings or 300 μm for whole-cell recordings) were cut perpendicularly to the long axis of the isolated hippocampus or sagittal to the midline of each hemisphere and allowed to recover for at least 1 h in a resting chamber, filled with gassed aCSF at room temperature (22–25°C).

fEPSP Recordings from CA3-CA1 Synapses

After at least 1 h recovery, individual slices were transferred to a recording chamber (1 + 5 mL dead volume) and continuously superfused at 3 mL/min with gassed aCSF at 32°C; the drugs were added to this superfusion solution. fEPSPs were recorded as previously described (Diógenes et al. 2004; Li, Ren et al. 2008) through an extracellular microelectrode (2–6 MΩ resistance) placed in the stratum radiatum of the CA1 area. Stimulation (rectangular 0.1 ms pulses, once every 15 s) was delivered through a concentric electrode placed on the Schaffer collateral–commissural fibers, in the stratum radiatum near the CA3-CA1 border. The intensity of stimulus (80–200 μA) was initially adjusted to obtain a large fEPSP slope with a minimum population spike contamination, being usually set to obtain an fEPSP slope of about 50% of the maximum. Slices were visualized with a dissection microscope and recordings were obtained with an Axoclamp 2B amplifier and digitized (Axon Instruments, Foster City, CA, United States of America). Individual responses were monitored, and averages of 8 consecutive responses were continuously stored on a personal computer with the LTP program (Anderson and Collingridge 2001). In some experiments and to allow comparisons between results obtained in mossy fiber synapses under the same experimental conditions, fEPSPs at the CA3-CA1 synapses were recorded using the same procedure as for recording fEPSPs at mossy fiber synapses (see below).

fEPSP Recordings from Mossy Fiber Synapses

Individual slices were transferred to the recording chamber (total fluid dead space: ~3 mL), maintained at 30–32°C, and constantly superfused at the rate of 1.5 mL/min. A concentric bipolar stimulating electrode was placed in the granule cell layer for mossy fiber fEPSPs. To confirm that the fEPSPs were mossy fiber in origin (2S,1′S,2′S)-2-(carboxycyclopropyl)glycine (LCCG-1, 10 μM), a selective antagonist of group II metabotropic glutamate receptors, was applied to the slice by a gravity-driven perfusion system at the end of each experiment (Kamiya et al. 1996). The recording microelectrode (0.5–1 MΩ) was positioned 200–600 μm from the stimulating electrode for recording orthodromically evoked fEPSPs. Stimuli consisted of 0.1 ms constant current square pulses, applied once every 20 s. The intensity of the stimulus was adjusted in each experiment to evoke about 50% of the maximal field potential amplitude without appreciable population spike contamination. Evoked responses were monitored online and stable fEPSP slope values were recorded for at least 10 min before increasing stimulation frequency to analyze frequency (1 Hz) facilitation of synaptic responses or paired-pulse facilitation (PPF). PPF was measured as the ratio between the second versus the first fEPSP slope responses at different interstimuli intervals (10–100 ms).

Slices were visualized with a Wild M3B microscope (Heerbrugg, Switzerland). fEPSPs were recorded and filtered (1 kHz) with an Axopatch 200 A amplifier (Axon Instruments) and digitized at 10 kHz with an A/D converter (Digidata 1322A, Axon Instruments). Data were stored on a computer using pClamp 9 software (Axon Instruments) and analyzed off-line with Clampfit 9 program (Axon Instruments). To allow comparisons between results obtained in mossy fiber synapses and CA1-CA3 synapses under the same experimental conditions, in some experiments, fEPSPs at these synapses were recorded using the same procedure as for recording fEPSPs at mossy fiber synapses, except that the stimulation electrode was placed in the stratum radiatum of the CA1 area.

Whole-Cell Recordings

Whole-cell patch-clamp recordings were performed on pyramidal neurons or interneurons at 21–23°C as described previously (Ragozzino et al. 2005). Membrane currents were recorded by using glass electrodes (3–4 MΩ), filled with K-gluconate 140 mM, HEPES 10 mM, 1,2-bis(2-aminophenoxy)ethane-*N*,*N*,*N*,*N*-tetraacetic acid 5 mM, $MgCl_2$ 2 mM, and Mg-ATP 2 mM (pH 7.35, with KOH) (Roseti et al. 2008). Under these experimental conditions, with inactivated voltage-gated channels, cells were stable and healthy for 1–2 h. Cells with depolarized resting membrane potential (greater than −50 mV) were discarded. GABA was delivered to cells by pressure applications (10–20 psi, 1 s; General Valve Picospritzer II) from glass micropipettes filled with 100 μM GABA, positioned above whole-cell voltage-clamped neurons. In this way, we obtained stable whole-cell currents and rapid drug wash before applying the repetitive application protocol. In order to observe the activity-dependent decrease in the currents mediated by $GABA_A$ receptors (I_{GABA}), the following repetitive application protocol was adopted: After current amplitude stabilization with repetitive applications every 120 s, a sequence of 10 GABA applications was delivered every 15 s, and the test pulse was resumed at the control rate (every 120 s) to monitor recovery of the GABA current. The reduction in peak amplitude current was expressed as residual current, that is, the percentage amplitude of current at the end of the repetitive application protocol versus control (10th I_{GABA}/1st I_{GABA}).

Quantification of Extracellular Purine Levels

Enzyme-based microelectrode biosensors were purchased from Sarissa Biomedical Ltd (Coventry, United Kingdom) and were used to detect extracellular levels of adenosine. The principle of their action and their use in hippocampal slices have been published previously, as have the protocols for slice preparation and simultaneous recordings of fEPSPs (Frenguelli et al. 2003; Etherington et al. 2009; Lopatar et al. 2011). Briefly, an enzymatic cascade (adenosine deaminase, nucleoside phosphorylase, xanthine oxidase) is entrapped in a polymer matrix surrounding a 50 µm platinum/iridium wire which is polarized to +600 mV. The polymer matrix adds ≤10 µm to the diameter of the Pt/Ir wire. Hydrogen peroxide produced by xanthine oxidase oxidizes on the Pt/Ir wire to give rise to a current proportional to the amount of purine released. Concentration units provided are µM′ to indicate that the signal from a sensor containing all 3 enzymes is a composite reflecting adenosine and its metabolites (Frenguelli et al. 2007; zur Nedden et al. 2011).

Pairs of sensors (ADO and NULL) were inserted into stratum radiatum of area CA1 of 400 µm parasagittal hippocampal slices maintained at 34°C. To allow sufficient time for slices to recover and the sensor signal to asymptote to a baseline level, an hour was left before the experiment commenced. Experiments consisted of (i) collecting 10 min of stable baseline; (ii) theta burst stimulation (TBS) protocol, (iii) 15 min of post-TBS recording, (iv) sensor withdrawal, and (v) sensor calibration. The TBS protocol consisted of 15 bursts of 4 pulses at 100 Hz separated by 200 ms, repeated 4 times at 10 s intervals. Since no signal was detected on null sensors in any of the experiments, null sensor traces were disregarded and only ADO traces were further processed. Upon sensor withdrawal, the ADO signal dropped below the preceding baseline level recorded in the slice. Subtraction of the pre- and postwithdrawal signals was used as an indirect measure of ADO tone. Calibration was carried out after each experiment by washing in adenosine (10 µM) and 5-hydroxytryptamine (5HT, 10 µM) with the latter used to test for patency of the permselective layer. Biosensor traces were smoothed with a 1 s average and are presented as mean release ± SEM. The area under curve for the first 5 min after TBS was used to quantify the release of adenosine upon TBS. Sensor signals were captured at 10 kHz using Spike 2 software, while the acquisition of fEPSPs was under the control of LTP software (Anderson and Collingridge 2001) as described previously (Frenguelli et al. 2007; zur Nedden et al. 2011).

Western Blotting

Sodium dodecyl sulfate (SDS)–polyacrylamide gel electrophoresis (PAGE) was used to evaluate the levels of TrkB receptors, ADK, AMPA (GluA1) and NMDA (GluN2B) subunits. For ADK evaluation, aqueous extracts of dorsal brain samples (hippocampus and dorsal cortex; $n = 5$–8 per group) were prepared by homogenizing and solubilizing the tissue in radioimmunoprecipitation assay buffer (Thermo Scientific, CA, United States of America) and by removing insolubilized material by centrifugation (104 × *g*, 15 min at 4°C). For TrkB receptor and AMPA (GluA1) and NMDA (GluN2B) subunit quantification, hippocampal homogenates ($n = 4$–8) were prepared as described before (Diógenes et al. 2007).

The protein content in the supernatants was determined using a commercial Bradford assay (Sigma, MO, United States of America). Twenty micrograms (for TrkB receptor evaluation), 50 µg (for ADK assessment), or 100 µg (for AMPA (GluA1) and NMDA (GluN2B) subunits) of protein extract were separated by electrophoresis on an SDS–10% PAGE gel and blotted onto a polyvinylidene fluoride membrane according to the standard procedures. The blots were probed for 1 h at room temperature with the polyclonal rabbit anti-ADK antibody or monoclonal mouse anti-TrkB (BD Transduction Laboratories) in 5% blocking reagent in TBST (10 mM Tris, 150 mM NaCl, 0.05% Tween 20 in H_2O). After washing (3 × 5 min in TBST), blots were then probed with secondary antibodies conjugated with horseradish peroxidase and bands were visualized with a commercial enhanced chemiluminescence detection method (ECL) kit (PerkinElmer Life Sciences, MA, United States of America). ADK levels were normalized to the α-tubulin loading control and reported relative to WT ADK (set as 100%). TrkB intensity values were normalized to the β-actin loading control and the relative intensities were normalized to WT (set as 100%). Densitometry of the bands was performed using the Image J processing software (NIH, MD, United States of America).

Immunohistochemistry

Adk-tg, Fb-Adk-def, and WT mice were anesthetized (3% isoflurane) and transcardially perfused with 0.15 M phosphate-buffered saline (PBS), followed by 4% paraformaldehyde in PBS. Brains were removed and postfixed in the same fixative at 4°C for 1 day before being cut into 40 µm coronal sections using a vibratome. Previously published procedures were used for the immunohistochemical detection of ADK (Studer et al. 2006). Digital images of ADK immunohistochemistry on 3,3′-diaminobenzidine (DAB)-stained slices were acquired using a Zeiss AxioPlan inverted microscope equipped with an AxioCam 1Cc1 camera (Carl Zeiss MicroImaging, Inc., Thornwood, NY, United States of America).

Drugs

BDNF was a kind gift of Regeneron Pharmaceuticals (Tarrytown, NY, United States of America) and was supplied in a 1.0 mg/mL stock solution in 150 mM NaCl, 10 mM sodium phosphate buffer, and 0.004% Tween 20. Adenosine and 5HT were purchased from Sigma (Sigma-Aldrich Company Ltd, Dorset, United Kingdom). 8-Cyclopentyl-1,3-dimethylxanthine (CPT) was from RBI (Poole, Dorset, United Kingdom). 7-(2-Phenylethyl)-5-amino-2-(2-furyl)-pyrazolo-[4,3-e]-1,2,4-triazolol[1,5-c]pyrimidine (SCH 58261), GABA, 9-chloro-2-(2-furanyl)-[1,2,4]triazolo[1,5-c]quinazolin-5-amine (CGS 15943), (2S,1′S,2′S)-2-(carboxycyclopropyl)glycine (LCCG-1), and 1,3-dipropyl-8-cyclopentyladenosine (DPCPX) were from Tocris Cookson (Ballwin, MO, United States of America). DPCPX was made up in a 5 mM stock solution in 99% dimethylsulfoxide (DMSO)–1 M 1% NaOH (v/v), SCH 58261 in a 10 mM stock solution in DMSO and CGS 15943 in a 5 mM stock solution in DMSO. Aliquots of these stock solutions were kept frozen at −20°C until use. The maximum amount of DMSO applied to the preparations (1/100 000 v/v) was devoid of effect on fEPSPs.

Data Analysis

Values are expressed as mean ± SEM. The significance of differences between means was evaluated by the Student's *t*-test or by one-way ANOVA with Bonferroni's correction for multiple comparisons. Values of $P < 0.05$ were considered to represent statistically significant differences.

Results

Regional Manipulation of ADK Expression in Transgenic Mice

These studies are based on transgenic mice with engineered regional changes of ADK expression in the brain. Adk-tg mice (Fedele et al. 2005; Li, Lan et al. 2008; Li, Ren et al. 2008) overexpress a constitutively expressed, loxP-flanked *Adk* transgene in lieu of the endogenous *Adk* gene, which is subject to dynamic expression changes (Gouder et al. 2004; Studer et al. 2006; Pignataro et al. 2008). As a result of the mutation, Adk-tg mice express spontaneous electrographic seizures and display lowered thresholds for seizure induction and for neuronal injury (Li et al. 2007; Pignataro et al. 2007; Li, Ren et al. 2008). Fb-Adk-def mice are identical to Adk-tg mice except for an *Emx1-Cre*-transgene-driven deletion of the *Adk* transgene in most cells of the dorsal telencephalon (Li, Lan et al. 2008; Li, Ren et al. 2008). As a result of this manipulation, Fb-Adk-def mice display increased thresholds for seizures and for neuronal injury (Li, Lan et al. 2008; Li, Ren et al.

2008; Pignataro et al. 2008), while they are resistant to the induction of epileptogenesis (Li, Lan et al. 2008; Li, Ren et al. 2008). These fundamental differences in susceptibility to seizures and to neuronal injury can be linked to differences in ADK expression in the forebrain including the hippocampus, but the underlying mechanisms have not yet been elucidated on a physiological level.

To demonstrate that the region-specific genetic manipulation of the *Adk* gene resulted in appropriate changes of ADK expression levels in the hippocampus, the expression of ADK was quantified by western blot analysis. The samples from young (3- to 5-week old) Fb-Adk-def mice showed a reduction in ADK levels to 48 ± 8.8% of WT ($n = 4$; $P < 0.05$; Fig. 1*A*), whereas the Adk-tg mice showed an increase in ADK to 163 ± 13% of WT ($n = 8$; $P < 0.01$). A similar pattern was obtained in samples prepared from adult (10- to 12-week old) Fb-Adk-def mice, where levels of ADK were reduced (62 ± 4.7%, $n = 6$; $P < 0.05$; Fig. 1*B*) in comparison to WT, whereas ADK expression in Adk-tg mice was increased to 187 ± 11.5% ($n = 7$; $P < 0.001$; Fig. 1*B*) of WT. ADK expression changes quantified in the western blot were matched by qualitative changes in ADK expression as seen by the evaluation of ADK immunoreactivity in peroxidase-stained hippocampal coronal sections. Inspection of the hippocampal formation revealed a region-specific decrease and increase in ADK expression in Fb-Adk-def and Adk-tg mice, respectively, compared with ADK expression in control WT mice (Fig. 1*C*). The ADK expression changes determined here were robust and stable across the age ranges investigated in subsequent experiments.

The Tone of Endogenous Adenosine is Governed by Expression Levels of ADK

The predominant influence of adenosine in the hippocampus is inhibition of synaptic transmission through A_1R activation (Sebastião et al. 1990). It is therefore possible to assess changes in extracellular adenosine levels in the vicinity of the synapses by evaluating the disinhibition of synaptic transmission caused by antagonism of the A_1R. The assumption is that higher levels of adenosine cause more pronounced tonic A_1R-mediated inhibition, and therefore, a higher facilitatory

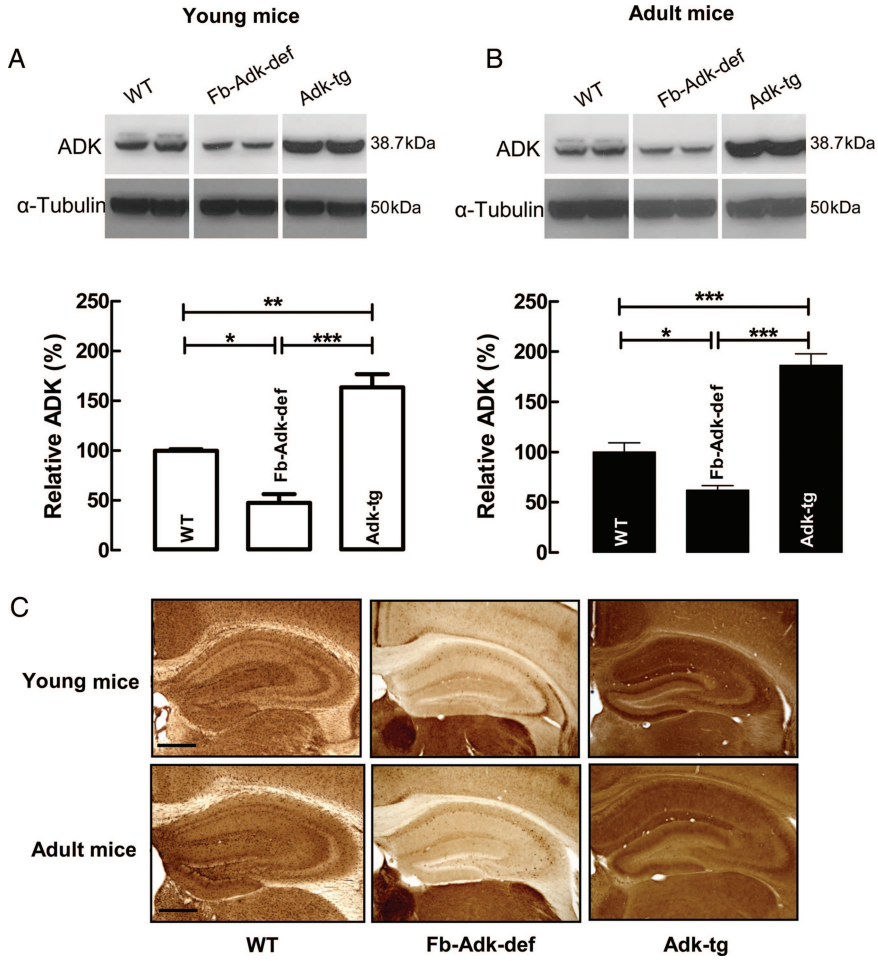

Figure 1. Genotype-specific ADK immunoreactivity in the mouse brain. (*A* and *B*) Western blot analysis of ADK immunoreactivity (38.7 kDa) from the hippocampus and dorsal cortex taken from young (*A*, 3–5 weeks old) or adult (*B*, 10–12 weeks old) mice. α-Tubulin immunoreactivity (50 kDa) was used as a loading control. The 3 different genotypes, WT, Fb-Adk-def, and Adk-tg, are indicated above each lane. Each blot shows data from 2 different animals of the same genotype and age. The quantitative analysis shows averaged data normalized to the loading control and to WT. Data were calculated based on multiple samples taken from different ages and genotypes (young: WT, $n = 5$; Fb-Adk-def, $n = 4$; Adk-tg, $n = 8$; adult: WT, $n = 6$; Fb-Adk-def, $n = 6$; Adk-tg, $n = 7$); data are presented as mean ± SEM. (*C*) Immunohistochemical analysis of coronal brain sections of the hippocampus from WT, Fb-Adk-def, and Adk-tg mice (young [upper panel] and adult [lower panel]); sections were stained with diaminobenzidine hydrochloride (DAB) for ADK immunoreactivity; scale bar: 500 μm. $^*P < 0.05$, $^{**}P < 0.01$, and $^{***}P < 0.001$ (one-way ANOVA with Bonferroni's multiple comparison test).

action of A_1R receptor antagonists should occur. The use of an A_1R antagonist to indirectly assess the extracellular levels of adenosine has the advantage of evaluating the synaptic adenosine influencing synaptic transmission. We therefore compared the effect of the selective A_1R antagonist, DPCPX, at a supramaximal concentration (50 nM, K_i value for DPCPX at the hippocampus ~0.5 nM; Sebastião et al. 1990) on synaptic transmission in hippocampal slices taken from young and adult WT, Fb-Adk-def, and Adk-tg mice.

In hippocampal slices taken from young WT mice, DPCPX (50 nM) increased the slope of fEPSP to 128 ± 4.2% ($n = 6$; Fig. 2*A*,*D*). In slices from Fb-Adk-def mice, DPCPX (50 nM) caused a significantly higher increase in fEPSPs (150 ± 7.6%, $n = 4$, $P < 0.05$; Fig. 2*B*,*D*) when compared with the effect observed in WT mice. This effect was also markedly higher than the effect detected in slices from Adk-tg mice (118 ± 4.1%, $n = 5$, $P < 0.05$; Fig. 2*C*,*D*). A similar genotypic influence occurred in hippocampal slices taken from adult mice, where DPCPX (50 nM) increased the slope of fEPSP to 145 ± 4.0% ($n = 7$) in WT (Fig. 2*A*,*D*), 181 ± 13.0% ($n = 4$, $P < 0.05$ vs. WT) in Fb-Adk-def mice (Fig. 2*B*,*D*) and 120 ± 6.5%, $n = 6$ ($P < 0.05$ vs. WT) in Adk-tg mice (Fig. 2*C*,*D*). As also shown in Figure 2*A*,*B*, the disinhibition caused by DPCPX in WT and Fb-Adk-def mice was significantly higher in adult than in young genotype-matched mice.

In summary, irrespective of age, the lowest disinhibition of synaptic transmission caused by DPCPX was observed in mice overexpressing ADK (Adk-tg), whereas the greatest disinhibition was found in adult mice underexpressing ADK (Fb-Adk-def). The data also show that adult WT mice had clearly greater ($P < 0.05$) A_1 inhibitory tone than young WT mice. These results demonstrate that both age and ADK activity determine tonic inhibition caused by adenosine at synapses.

Direct Measurement of Basal and TBS-Evoked Purine Release

The previous results indicate differences in basal adenosine levels across the 3 genotypes. To determine whether activity-dependent release of adenosine was similarly dependent upon the expression level of ADK, we delivered 4 periods of TBS (15 bursts of 4 pulses at 100 Hz separated by 200 ms, repeated 4 times at 10 s intervals) to the afferent Schaffer collateral–commissural pathway of hippocampal slices taken from adult mice of the 3 genotypes. We have recently shown that repeated TBS is an effective stimulus for adenosine release in CA1 area (zur Nedden et al. 2011). As quantified with adenosine biosensors (Fig. 3), TBS resulted in robust adenosine release in slices from WT mice (0.97 ± 0.14 μM′ min, $n = 5$; Fig. 3*A*), which was associated with a transient (~2 min) depression of the fEPSP and a subsequent sustained potentiation (166 ± 13% at 15 min; Fig 3*A*).

To establish whether the transient depression of the fEPSP in response to TBS reflected adenosine release and the activation of adenosine A_1R, TBS was delivered in the presence or absence of the adenosine A_1R antagonist 8-CPT (1 μM). In the absence of 8-CPT, the fEPSP was depressed by 31 ± 12% of control 15 s after the last TBS ($n = 8$ slices from 4 WT

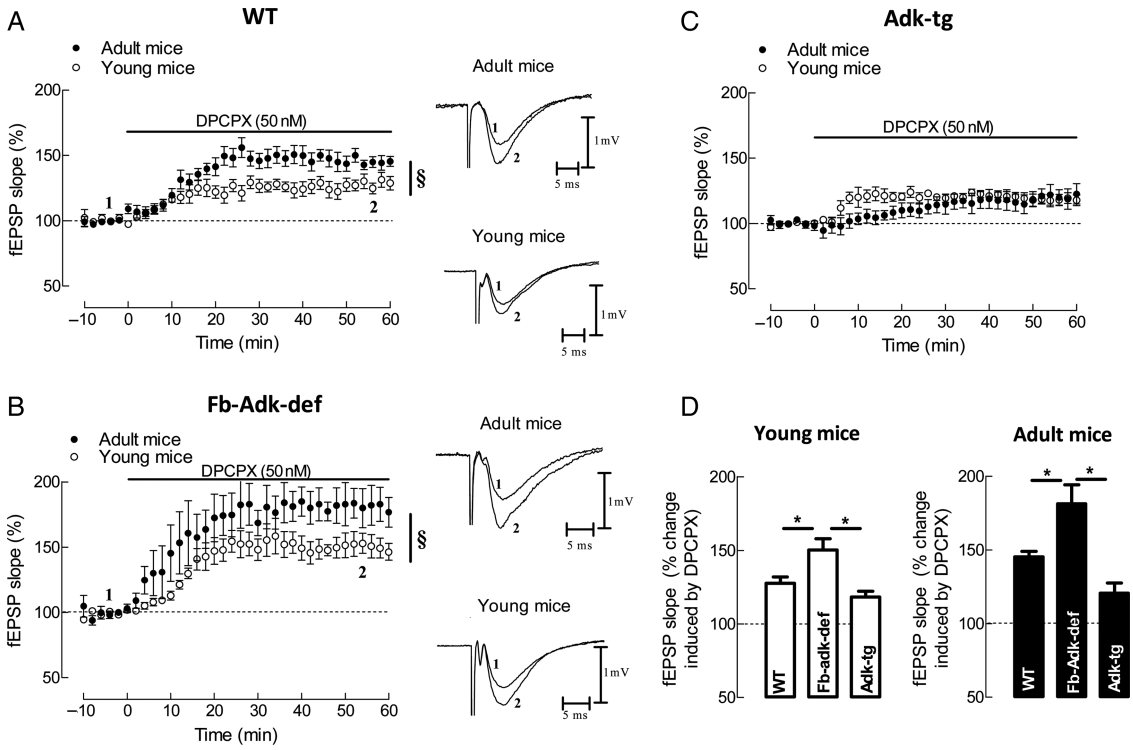

Figure 2. Influence of genotype upon A_1R-mediated tonic inhibition of synaptic transmission at CA3/CA1 hippocampal synapses. The selective A_1R antagonist, DPCPX (50 nM) was used to block A_1R-mediated tonic inhibition of synaptic transmission. (*A*–*C*) Averaged time courses of changes in fEPSP slope induced by application of DPCPX in slices taken from young (*A*, open circle, $n = 6$) and adult (*A*, filled circle, $n = 7$) WT, young (*B*, open circle, $n = 4$) and adult (*B*, filled circle, $n = 4$) Fb-Adk-def mice, and young (*C*, open circle, $n = 5$) and adult (*C*, filled circle, $n = 6$) Adk-tg mice. Right panels in (*A*) and (*B*) show illustrative fEPSP traces obtained immediately before (1) and during (2) DPCPX application; each trace is the average of 8 consecutive responses and the fEPSP is preceded by the stimulus artifact and the presynaptic volley; the stimulus artifact has been truncated in amplitude. (*D*) Comparison of the averaged effects of DPCPX in the different genotypes within each age group. $^{§}P < 0.05$ (Student's *t*-test) and $^{*}P < 0.05$ (one-way ANOVA with Bonferroni's multiple comparison test).

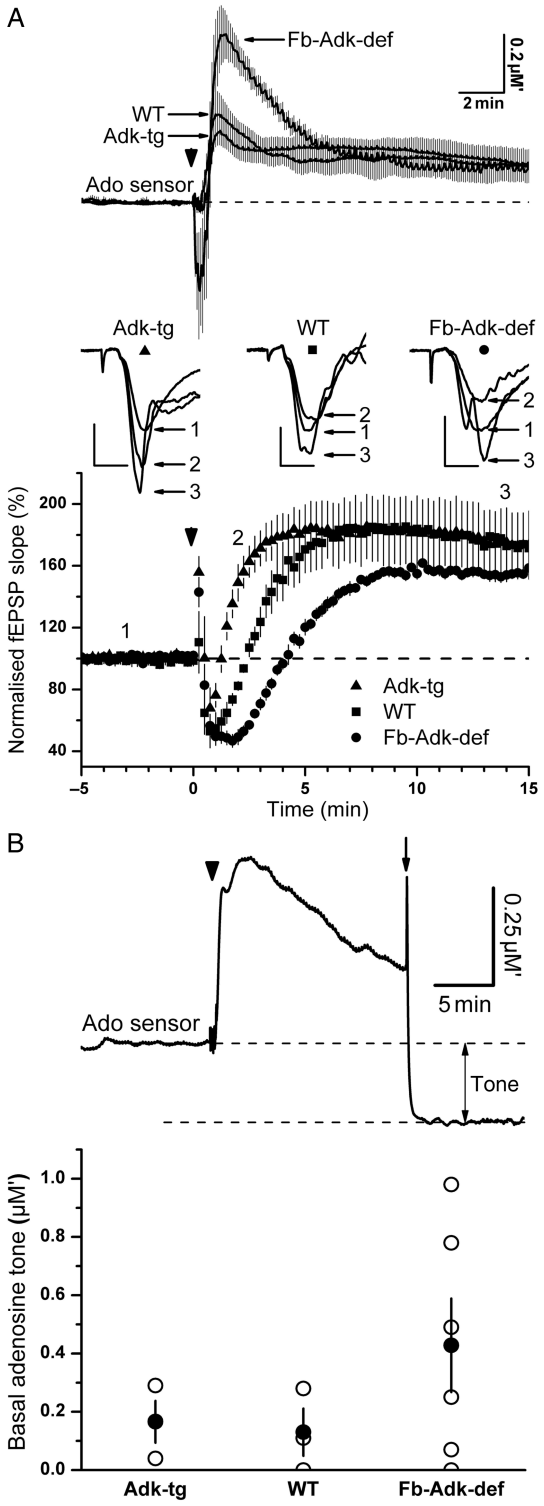

Figure 3. Influence of genotype upon the basal and activity-dependent increase in extracellular adenosine levels, as measured with a microelectrode adenosine biosensor. (*A*) Upper panel, adenosine release in response to repeated TBS (15 bursts of 4 pulses at 100 Hz separated by 200 ms, repeated 4 times at 10 s intervals; arrowhead) in slices from WT ($n = 5$), Fb-Adk-def ($n = 8$), and Adk-tg ($n = 6$) mice. Note much greater release of adenosine in slices from mice deficient in ADK and reduced peak adenosine release in slices from mice overexpressing ADK. Traces represent mean ± SEM. Lower panel, the time course of simultaneously recorded fEPSPs from the experiments shown in the upper panel. TBS at time zero resulted in a transient depression of the fEPSP in WT slices (squares, $n = 5$), which was longer in slices from mice deficient in ADK (circles, $n = 8$), likely reflecting enhanced release of adenosine (upper traces), while the depression was shorter lasting in slices overexpressing ADK (triangles, $n = 6$). Inset are fEPSPs from the 3 genotypes taken at the times indicated by the numbers 1, 2, and 3 before TBS, ~2 min after TBS, and ~14 min after TBS, respectively. Note at 2 min, the individual fEPSPs reflect the pooled data demonstrating (from left to right): The enhancement of the fEPSP in Adk-tg slices above the preceding control fEPSPs, return of WT fEPSPs to close to control, and continued depression of fEPSPs from Fb-Adk-def slices relative to control fEPSPs. Symbols below the genotype refer to the corresponding traces in the fEPSP time course plot. Scale bars for fEPSPs measure 0.5 mV and 5 ms. (*B*) Upper trace shows the representative experiment of basal tone measurement where the adenosine sensor was removed from the slice (arrow) 15 min after TBS (arrowhead). The difference between the preceding sensor baseline and the background sensor current is taken as an estimate of the basal adenosine tone. The lower bar graph provides the mean ± SEM (filled circle) and individual tone measurements (open circles) from WT ($n = 3$), Adk-tg ($n = 3$), and Fb-Adk-def ($n = 6$) slices. Values of adenosine are provided in $\mu M'$ to indicate that this is a composite signal reflecting adenosine and its metabolites (inosine and hypoxanthine).

mice). In contrast, in slices pretreated with 8-CPT, the transient depression was absent and instead a potentiation (129 ± 10% of baseline) was observed 15 s after the end of TBS ($n = 5$ slices from 3 WT mice). Thus, the release of adenosine during TBS has functional consequences in causing a transient depression of synaptic transmission via the activation of adenosine A_1R.

Consistent with the concept of ADK regulating the release of adenosine in response to high-frequency network activity, slices from Fb-Adk-def mice showed greater adenosine release (1.63 ± 0.27 μM′ min, $n = 8$), longer post-TBS depression of synaptic transmission (~4 min), and a weaker potentiation of the fEPSP (159 ± 3% at 15 min post-TBS). In contrast, overexpression of ADK resulted in a brief transient depression of the fEPSP, which recovered ~75 s after stimulation, and lower levels of adenosine release (0.82 ± 0.16 μM′ min, $n = 6$) (Fig. 3*A*).

In a subset of these experiments, the adenosine biosensor was removed 15 min after TBS to provide an estimate of the basal adenosine tone, which we interpret as the difference between the sensor current when removed from the slice relative to the pre-TBS baseline (Fig 3*B*). In contrast to the differential effects on fEPSPs obtained with the adenosine A_1R antagonist between WT and Adk-tg slices, there was little difference between WT and Adk-tg slices in terms of the basal tone as measured with the adenosine biosensors (0.13 ± 0.08 μM′, $n = 3$; 0.17 ± 0.07 μM′, $n = 3$, respectively). However, Fb-Adk-def slices showed a tendency towards substantially greater basal adenosine (0.43 ± 0.16 μM′, $n = 6$), but this did not reach statistical significant, due to considerable variability in individual measurements of basal tone (Fig. 3*B*). This likely stems from the difficultly in ascribing absolute measurements of background current (and hence basal adenosine concentration) based upon removal of the sensor from the slice.

The above data suggest that ADK has an important role in regulating activity-dependent release of adenosine, which may set the threshold for homeostatic network interactions among a variety of neurotransmitter and neuromodulatory systems.

Variation in ADK Expression Levels Correlates with Differential Short-Term Synaptic Plasticity at Low Release Probability Hippocampal Synapses

We next evaluated how variations in ADK expression could affect functioning of low release probability synapses, such as the mossy fiber synapses. It has been a matter of debate if the low release probability of mossy fiber synapses could result

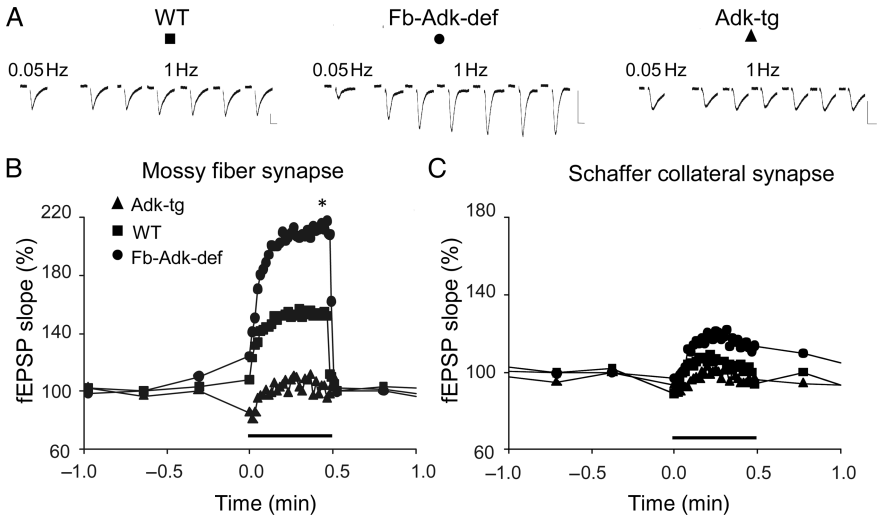

Figure 4. Frequency facilitation depends on ADK level at mossy fiber but not at Schaffer collateral synapses. (*A* and *B*) 1-Hz facilitation at mossy fibers in hippocampal slices. (*A*) Representative traces recorded during 0.05 and 1 Hz stimulation (one every 5 s), as indicated, in WT, Fb-Adk-def, and Adk-tg. Vertical bars: 2 mV, horizontal bars: 10 ms. (*B*) The average time course of fEPSP slope from WT (filled square, $n = 6$), Fb-Adk-def (filled circle, $n = 6$), and Adk-tg (filled triangle, $n = 6$) mice, as indicated. At the time indicated by the horizontal bar, stimulus frequency was increased from 0.05 to 1 Hz for 30 s. (*C*) Average time course of 1-Hz fEPSP slope facilitation at Schaffer collateral synapse for the same genotypes as indicated in (*B*) ($n = 4$ for each genotype); symbols as in (*B*); note the limited facilitation following 1-Hz stimulation, in contrast with the facilitation shown in (*A* and *B*). *$P < 0.05$, Fb-Adk-def versus Adk-tg (Student's *t*-test).

from A_1R-mediated tonic inhibition by ambient adenosine levels, though discordant data on adenosine contribution have been reported (Moore et al. 2003; Kukley et al. 2005). As a consequence of low release probability, hippocampal mossy fiber synapses show 2 main characteristics: 1) A remarkable frequency facilitation, for which the increase in stimulation frequency from a low rate (e.g. 0.05 Hz) to a modest rate (e.g. 1 Hz) markedly enhances transmission, an enhancement fully blocked by DPCPX, therefore A_1R-dependent (Moore et al. 2003); and 2) a pronounced PPF, where the second response to 2 closely timed stimuli is enhanced, a process also highly sensitive to A_1R blockade (Moore et al. 2003). We hypothesized that at these synapses, a variation of the level of adenosine could modify the magnitude of those short-term synaptic plasticity events. Baseline synaptic responses induced by low-frequency (0.05 Hz) stimulation were recorded continuously and then the frequency was increased to 1 Hz for 30 s, as indicated in Figure 4. Immediately after this brief and moderate increase in stimulation frequency, fEPSPs in mossy fiber synapses rapidly increased and recovered upon return to basal stimulus frequency (Fig. 4*A*,*B*). Interestingly, in the Fb-Adk-def mice, where the absence of ADK produces an increase in ambient levels of adenosine, the average maximal frequency facilitation was significantly ($P < 0.05$) larger ($211 \pm 60\%$ of fEPSP slope increase, $n = 6$) than in Adk-tg mice ($103 \pm 40\%$, $n = 6$; $P < 0.05$). In WT animals, the average maximal frequency facilitation was 155 ± 36 ($n = 6$). As expected, the effect of ambient adenosine on short-term plasticity induced by 1 Hz stimulation for 30 s was more prominent on mossy fibers (Fig. 4*A*,*B*) compared with Schaffer collateral synapses (Fig. 4*C*), where no significant difference between different genotypes was observed, though a similar genotype-specific pattern occurred.

We next evaluated another type of short-term synaptic plasticity, paired pulse facilitation (PPF), which was measured at different interstimuli intervals ranging from 10 to 100 ms (Fig. 5). Again, we observed a larger facilitation in Fb-Adk-def

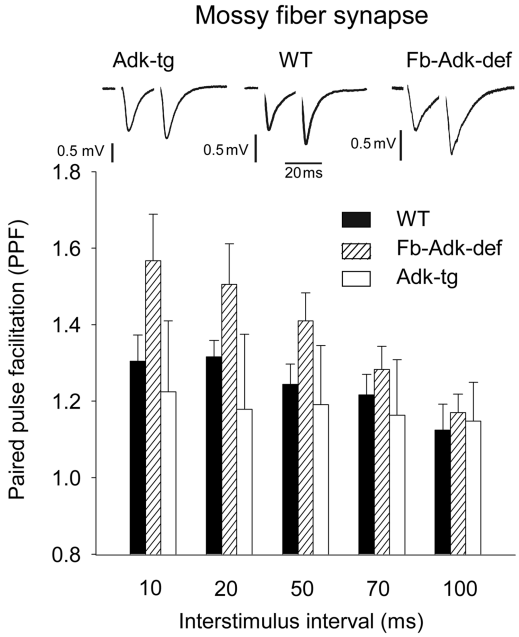

Figure 5. ADK expression influences PPF at mossy fiber synapses. PPF measured at different interstimuli intervals. (Upper panel) Typical traces recorded at 20 ms of interstimulus in the different genotypes, as indicated. Vertical bars: 0.5 mV, horizontal bar: 20 ms. (Lower panel) Histograms of PPF at interstimulus of 10, 20, 50, 70, and 100 ms. The ordinates refer to an average value of PPF measured as a ratio between the second and the first fEPSP slope responses in hippocampal slices from WT ($n = 7$), Fb-Adk-def ($n = 7$), and Adk-tg ($n = 5$) mice, as indicated.

mice ($n = 7$) compared with WT ($n = 7$), or Adk-tg mice ($n = 5$), the difference being particularly evident for lower interstimuli intervals. In order to quantify how much the genetically modified mice differ from the WT, we computed the mean and the variance of the WT data for each interstimulus interval. Then we calculated the probability (*P*-value) that

data from modified mice fit a Gaussian distribution with the WT mean and variance. The obtained *P*-value was lower than 0.0001 for either Fb-Adk-def or Adk-tg mice, thus fully rejecting the hypothesis that the PPF in Fb-Adk-def and Adk-tg mice were similar to PPF in WT. These data suggest that ADK expression affects the probability of transmitter release and hence directly influences the extent of short-term synaptic plasticity at mossy fiber synapses.

Variation in ADK Expression Removes the Influence of Age upon the Facilitatory Action of BDNF on Synaptic Transmission

In adult animals, BDNF has an excitatory effect upon synaptic transmission which is dependent on tonic $A_{2A}R$ activation by endogenous adenosine (Diógenes et al. 2007; Tebano et al. 2008). To establish whether this $A_{2A}R$-mediated action of endogenous adenosine in the hippocampus could also be affected by manipulation of ADK expression, we compared the effect of BDNF on fEPSPs from slices taken from mice of the 3 genotypes (WT, Adk-tg, and Fb-Adk-def mice). Remarkably, in adult mice overexpressing ADK (Adk-tg), the effect of BDNF (20 ng/mL) was completely lost ($n = 6$; Fig. 6*C*,*D*), whereas in WT mice, BDNF (20 ng/mL) caused the expected enhancement of fEPSP slope (to 128 ± 7.6%, $n = 7$, $P < 0.05$; Fig. 6*A*,*D*). Interestingly, this increase was not significantly different ($P > 0.05$; Fig. 6*D*) from that observed in slices from Fb-Adk-def mice (140 ± 9.7%, $n = 5$; Fig. 6*B*,*D*).

It has been suggested that variations in tonic activation of $A_{2A}R$ by endogenous adenosine relates to the age-dependency of the effect of BDNF upon synaptic transmission (Diógenes et al. 2007). To test this hypothesis, we evaluated the effect of BDNF in young (3–5 weeks old) mice of the 3 genotypes to allow comparisons with data obtained in genotype-matched adults. We first evaluated whether the increased levels of extracellular adenosine in Fb-Adk-def mice were enough to trigger the effects of BDNF in young mice. Remarkably, in these ADK-deficient animals, BDNF (20 ng/mL) significantly increased the fEPSP slope to 135 ± 7.2% ($n = 9$, $P < 0.05$; Fig. 6*F*,*H*). In contrast, BDNF (20 ng/mL) did not significantly influence ($n = 8$, $P > 0.05$) fEPSPs when applied to hippocampal slices taken from WT mice (Fig. 6*E*,*H*) or when applied to slices from mice overexpressing ADK in the forebrain (Adk-tg mice) ($n = 6$; Fig. 6*G*,*H*).

The above results show that BDNF-induced facilitation of hippocampal synaptic transmission is lost under high ADK levels and that under reduced ADK levels, the BDNF facilitatory action becomes independent of age. Furthermore, whenever an effect of BDNF upon fEPSPs was seen, it was prevented by the selective $A_{2A}R$ antagonist, SCH 58261 (50 nM; Fig. 6*A*,*B*,*F*). These data demonstrate ADK as an upstream regulator of an $A_{2A}R$-dependent facilitatory action of BDNF.

Since the excitatory actions of BDNF are mediated by the activation of its full-length (FL) TrkB receptor isoform (TrkB-FL), the above ADK-dependent effects of BDNF could be due to changes in TrkB-FL expression. Moreover, ADK is largely expressed in astrocytes, which express a dominant-negative isoform of TrkB (TrkB.T1). Therefore, the levels of TrkB-FL and TrkB.T1 in hippocampal slices were evaluated by western blotting. Neither TrkB-FL nor TrkB.T1 levels were significantly ($P > 0.05$) different in the 3 genotypes (WT, Fb-Adk-def, and Adk-tg). In addition, and since the effects of BDNF upon basal synaptic transmission are dependent on NMDA receptor activation (Diógenes et al. 2007), we evaluated whether changes in BDNF effects observed in the 3 genotypes could be due to changes in glutamate receptor expression. As assessed by western blotting, AMPA (GluA1) subunits and NMDA (GluN2B) subunit levels did not differ significantly ($P > 0.05$) in the 3 genotypes (WT, Fb-Adk-def, and Adk-tg). Therefore, the genotype dependency of the synaptic actions of BDNF, described above, cannot be attributed to alterations in the levels of BDNF receptors or glutamate receptors.

ADK Expression Influences the I_{GABA} Stability in CA3 Pyramidal Neurons

While facilitation of BDNF actions by adenosine is clearly an $A_{2A}R$-mediated response and inhibition of synaptic transmission and release probability by adenosine are clearly A_1R-mediated responses, the modulation of the stability of $GABA_A$ receptor-mediated currents (I_{GABA}) by adenosine results from the activation of non-A_1 adenosine receptors (Sebastião 2010) and may involve $A_{2A}R$ and A_3 receptors (A_3R) (Roseti et al. 2008, 2009). In order to evaluate how changes in ambient adenosine would also affect these less explored actions of adenosine, with an obvious impact upon the hippocampal inhibitory signaling pathways, we analyzed the stability of I_{GABA} upon repetitive GABA application to hippocampal neurons in WT, Adk-tg, and Fb-Adk-def mice. CA3 hippocampal neurons were identified as pyramidal or non-pyramidal (interneurons) by shape and electrophysiological characterization of action potential properties (Fig. 7*A*,*B*) (Lacaille et al. 1987; Chitwood and Jaffe 1998).

The local pressure application of GABA (100 μM; 1 s) evoked outward whole-cell currents (I_{GABA}) on all tested cells (Fig. 7*C*,*D*,*E*). The current amplitudes in response to the first application of GABA were 2020 ± 280 pA ($n = 11$), 530 ± 150 pA ($n = 7$), and 1130 ± 280 pA ($n = 7$) for pyramidal neurons of WT, Fb-Adk-def, and Adk-tg mice, respectively. The first application of GABA evoked currents on interneurons of 910 ± 130, 1100 ± 300, and 1290 ± 120 pA for WT, Fb-Adk-def, and Adk-tg mice, respectively. There were no significant differences between current amplitudes evoked by the first application of GABA in WT or Adk mutant mice. Upon repetitive GABA applications, I_{GABA} amplitudes significantly decreased (Fig. 7*C*,*D*,*E*) in all tested cells. That this rundown of I_{GABA} was at least in part regulated by adenosine is suggested by the observation that for Adk-tg pyramidal neurons, the rundown of I_{GABA} after repeated GABA applications was significantly less (21 ± 4% inhibition, $n = 7$) than for WT pyramidal neurons (40 ± 2% inhibition, $n = 11$; $P < 0.05$; Fig. 7*C*), while for Fb-Adk-def pyramidal neurons, the rundown of I_{GABA} tended to be even greater (49 ± 4% inhibition, $n = 7$; Fig. 7*C*). In contrast, the activity-dependent rundown of I_{GABA} was not different across genotypes in interneurons, being 36 ± 6% ($n = 7$), 42 ± 6% ($n = 8$), and 32 ± 4% ($n = 7$) inhibition for WT, Fb-Adk-def, and Adk-tg mice, respectively (Fig. 7*D*). These data suggest a pyramidal neuron-specific action of adenosine and its regulation by ADK.

Independent confirmation of the role of adenosine receptors in the stability of I_{GABA} in pyramidal neurons was obtained in a separate series of experiments using the non-selective adenosine receptor antagonist, CGS 15943,

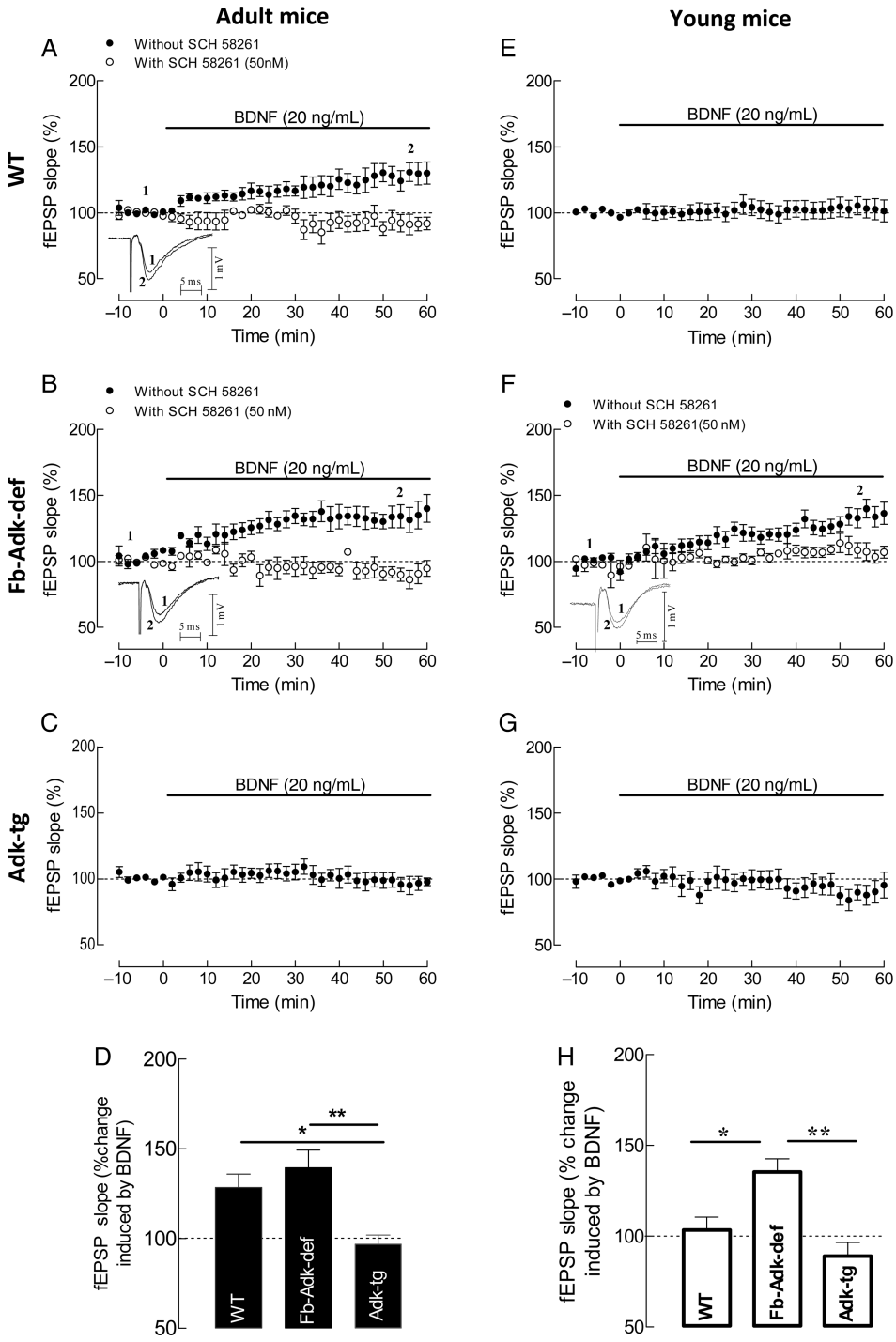

Figure 6. ADK expression influences A_{2A}R-dependent facilitatory effect of BDNF on synaptic transmission depending on the age of the animals. (*A–C* and *E–G*) Averaged time courses of changes in fEPSP slope induced by application of 20 ng/mL (corresponding to ~0.8 nM) BDNF in slices taken from 10- to 12-week WT (*A*, filled circle, $n = 7$), Fb-Adk-def (*B*, filled circle, $n = 5$), and Adk-tg (*C*, filled circle, $n = 6$) mice or from 3- to 5-week WT (*E*, filled circle, $n = 8$), Fb-Adk-def (*F*, filled circle, $n = 9$), and Adk-tg (*G*, filled circle, $n = 6$) mice. *A* (open circle, $n = 5$), *B* (open circle, $n = 4$), and *F* (open circle, $n = 6$) also illustrate the blockade of the effect of BDNF upon the blockade of A_{2A}R with the selective antagonist, SCH 58261 (50 nM), which by itself did not influence fEPSPs, as it did not affect the absence of the effect of BDNF in hippocampal slices from Fb-Adk-tg mice. *A*, *B*, and *F*, as an inset of the time course graph, are shown illustrative fEPSP traces obtained immediately before (1) and during (2) BDNF application; each trace is the average of 8 consecutive responses and the fEPSP is preceded by the stimulus artifact and the presynaptic volley; the stimulus artifact has been truncated in amplitude. (*D* and *H*) Comparison of the averaged effects of BDNF (change in fEPSP slope at 50–60 min) in the different genotypes in relation to pre-BDNF values (100%) from experiments shown in (*A–C*) and (*E–G*) as indicated in each column. All values are mean ± SEM. $^*P < 0.05$ and $^{**}P < 0.001$ (one-way ANOVA with Bonferroni's multiple comparison test).

known to reduce the I_{GABA} rundown in human and rat cortical pyramidal neurons as well as in cortical pyramidal neurons from $A1^{-/-}$ mice (Roseti et al. 2008). In the presence of CGS 15943 (100 nM), the activity-dependent rundown of I_{GABA} in Fb-Adk-def pyramidal neurons was significantly reduced from 41 ± 3 to 24 ± 4% inhibition ($n = 7$; $P < 0.05$; Fig. 7*E*), a value similar to that observed in Adk-tg neurons (Fig. 7*C*), clearly indicating that the differences observed in I_{GABA} stability in

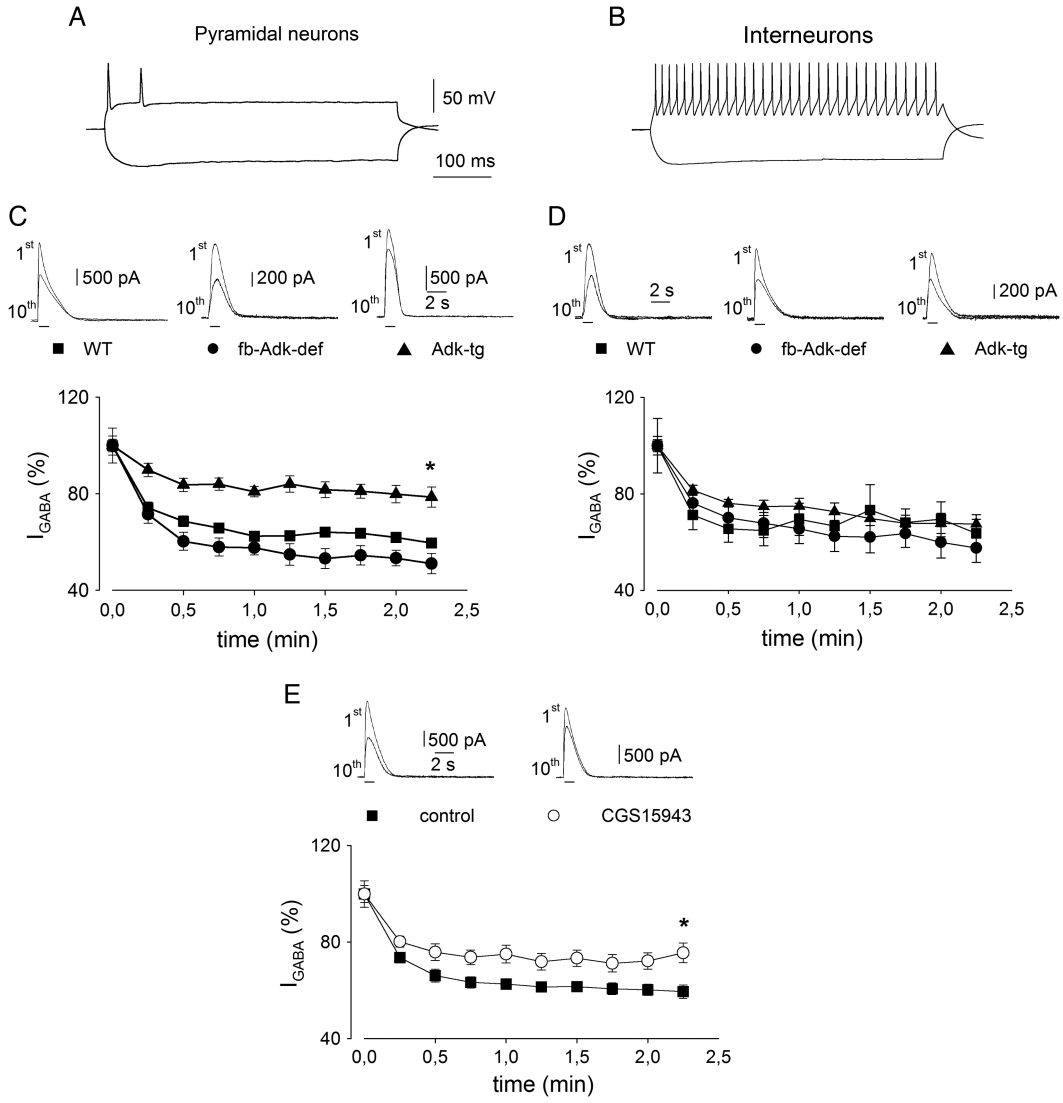

Figure 7. High ADK expression is associated with increased I_{GABA} stability upon repetitive GABA application on CA3 pyramidal neurons. (*A*) Typical trace showing action potential properties in a current-clamped WT CA3 pyramidal neuron. Note the marked action potential accommodation. Current intensity: 100 pA. (*B*) Typical trace showing action potential properties in a current-clamped WT CA3 interneuron. Current intensity, 100 pA. Note lack of accommodation and marked after hyperpolarization. (*C*) (Top) Typical traces showing 1st and 10th I_{GABA} evoked by repetitive pressure application of 100 μM GABA (horizontal bars; 0 mV holding potential) in WT (filled square), Fb-Adk-def (filled circle), and Adk-tg (filled triangle) CA3 pyramidal neurons, as indicated. (Bottom) Average time courses of I_{GABA} evoked by repetitive GABA applications (1 s duration every 15 s), in WT ($n = 11$), Fb-Adk-def ($n = 7$), and Adk-tg ($n = 7$) CA3 pyramidal neurons, as indicated. Note higher I_{GABA} stability significantly associated with Adk-tg neurons ($P < 0.05$). (*D*) (Top) Typical traces showing 1st and 10th I_{GABA} evoked by repetitive application of GABA in WT (filled square), Fb-Adk-def (filled circle), and Adk-tg (filled triangle) CA3 interneurons, as indicated. (Bottom) Average time courses of I_{GABA} evoked by repetitive GABA applications in WT ($n = 7$), Fb-Adk-def ($n = 8$), and Adk-tg ($n = 7$) CA3 interneurons, as indicated. (*E*) The blockade of adenosine receptors inhibits the activity-dependent I_{GABA} decrease in Fb-Adk-def CA3 pyramidal neurons. (Top) Typical traces showing 1st and 10th I_{GABA} evoked by repetitive pressure application of GABA 100 μM (horizontal bars; 0 mV holding potential) before (filled circle) and during (open circle) the application of the adenosine receptors blocker CGS 15943 100 nM, as indicated. (Bottom) Average time courses of I_{GABA} evoked by repetitive GABA applications observed in the same cells before (filled circle, $n = 7$) and during (open circle) the administration of CGS 15943. Note higher I_{GABA} stability in the presence of CGS 15943 ($P < 0.05$).

different ADK-expressing mice are mediated by adenosine acting on its receptors.

These data therefore show that reduced activation of adenosine receptors via either Adk-tg-mediated low ambient levels of adenosine or the antagonism of adenosine receptors increases the stability of I_{GABA} at pyramidal cells, not in interneurons.

Discussion

Here, we demonstrate that ADK, by regulating the extracellular tone of adenosine, exerts upstream control over 3 major adenosine-dependent pathways (Fig. 8): 1) A_1R-dependent inhibition of synaptic transmission and plasticity, 2) A_{2A} R-dependent promotion of BDNF-signaling, and 3) adenosine receptor-dependent modulation of GABAergic currents. Together, these properties of adenosine regulate fundamental aspects of both inhibitory and excitatory synaptic transmission in the mammalian brain. By virtue of setting an extracellular tone of adenosine permissive to such modulation, ADK therefore exerts major upstream control of both the strength and dynamic range of synapses.

ADK-Dependent Control of Synaptic Transmission and Plasticity

Studies using adenosine-sensitive biosensors revealed a tendency toward a larger background current in hippocampal

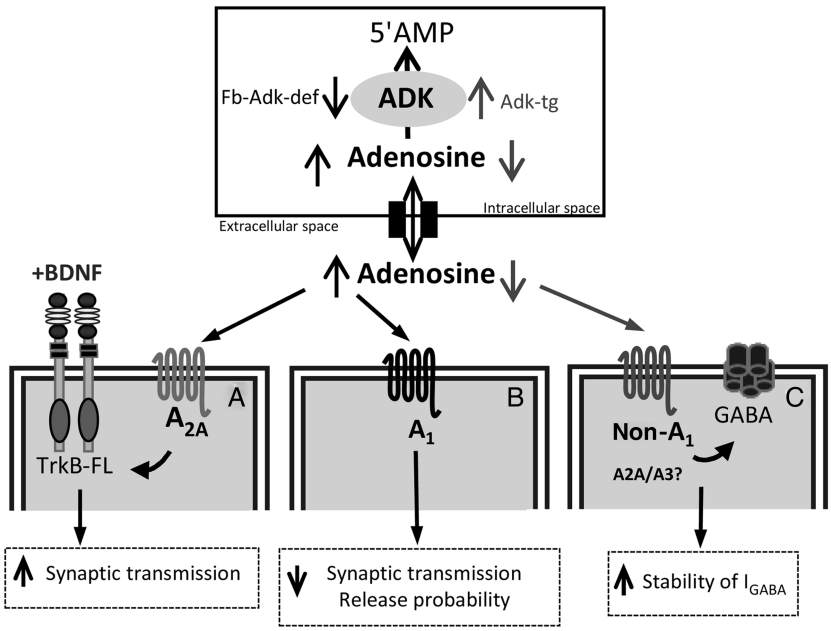

Figure 8. Schematic diagram summarizing the main conclusion that regulation of endogenous adenosine tone by adenosine kinase exerts homeostatic control over synaptic activity. ADK, by phosphorylating intracellular adenosine to 5′AMP, maintains an inward adenosine gradient, driving adenosine influx into the cell. When ADK levels are increased (Adk-tg mice), adenosine levels decrease, whereas reduced ADK levels (Fb-Adk-def) lead to increased extracellular adenosine concentration. ADK, by regulating the extracellular tone of adenosine, exerts upstream control over 3 major adenosine-dependent pathways: (*A*) A_{2A}R-dependent promotion of BDNF-signaling, (*B*) A_1R-dependent inhibition of synaptic transmission and plasticity, and (*C*) adenosine receptor-dependent modulation of GABAergic currents. When animals have reduced levels of ADK (Fb-ADK-def), the increased levels of adenosine facilitate BDNF actions upon synaptic transmission through the activation of A_{2A}R (*A*) and inhibit synaptic transmission through A_1R (*B*), this inhibition leading to a marked enhancement of short-term synaptic plasticity at low release probability synapses. When ADK levels are increased (Adk-tg), the decreased levels of adenosine increase the stability of I_{GABA} via non-A1R (*C*).

slices from Fb-Adk-def mice. Although the sensors are also sensitive to inosine and hypoxanthine, this increased signal is consistent with the evidence obtained by independent means for elevated extracellular adenosine levels. Accordingly, in comparison to Adk-tg mice and to WT controls, Fb-Adk-def animals have the highest adenosinergic inhibitory tone in their hippocampus as demonstrated by: 1) The highest degree of disinhibition of synaptic transmission by A_1R blockade, 2) the prolonged duration of the transient inhibition of fEPSPs immediately after TBS stimulation, 3) the delayed enhancement of fEPSPs after TBS stimulation in high release probability synapses, such as the CA1 pyramidal synapses, and 4) the highest frequency-dependent facilitation in low release probability synapses, such as the mossy fiber synapses. These findings are in accordance with the predominant expression of the A_1R in the hippocampus (Sebastião and Ribeiro 2009) and clearly show that ADK activity is a key upstream controller of the degree of modulation exerted by adenosine at A_1Rs. It also suggests that despite the high affinity of these receptors for its endogenous ligand, receptor occupancy is submaximal in WT animals. Age also appears to influence adenosinergic tonus in WT animals, since disinhibition of synaptic transmission caused by A_1R blockade was more pronounced in adult than in young mice. This suggests increased adenosine-mediated tone in older animals, which likely explains the adenosine-, age-, and locus-dependent modulation of LTP in rat CA1 pyramidal neurons (Rex et al. 2005; Diógenes et al. 2011).

Upon low-frequency stimulation, the adenosinergic inhibitory tonus in Adk-tg mice was not significantly different from that in WT mice, as assessed by the effect of DPCPX on synaptic transmission. Similarly, when directly measuring the basal adenosine levels with an adenosine-sensitive sensor, no difference between slices from WT and Adk-tg mice was obtained. In contrast, clear differences between these 2 genotypes were seen when high-frequency stimulation paradigms were used, suggesting that the impact of ADK activity upon tonic inhibition is particularly relevant upon high-frequency neuronal firing, where the extracellular accumulation of adenosine is clearly inversely related with ADK activity. It is worthwhile to note that ADK in WT mice is largely expressed in astrocytes rather than in neurons (Studer et al. 2006). One has therefore to conclude that astrocytes both control extracellular adenosine levels and sense neuronal activity in a concerted way. A possibility is that the higher the ADK activity, the lower the intracellular adenosine concentration in astrocytes, thereby reducing the quantity of adenosine available for release. However, this hypothesis does not explain how adenosine release from astrocytes is controlled by neuronal firing, unless one postulates astrocytic adenosine release provoked by neuronal glutamate exocytosis, an unlikely possibility since there is recent evidence that the source of adenosine depressing neuronal activity during excessive firing is predominantly neuronal rather than astrocytic (Lovatt et al. 2012). Alternatively, astrocytes may act as a sink of purines released by neurons, so that the higher the ADK activity (Adk-tg), the higher the adenosine concentration gradient across the astrocytic membrane, therefore the higher the amounts of adenosine taken up. Conversely, the lower the ADK activity (Fb-Adk-def) is, the lower the adenosine gradient across the astrocytic membrane, the lower the amounts of adenosine taken up, and the higher the net extracellular

adenosine levels. This mechanism would be particularly evident during intense neuronal firing leading to increased accumulation of synaptic adenosine. Regardless of the underlying mechanism, a major conclusion from the present work is that ADK activity in astrocytes controls extracellular levels of adenosine in a neuronal activity-dependent manner, playing a pivotal role in astrocyte-to-neuron communication and likely contributing to negative feedback regulation of neuronal firing to avoid entry into aberrant states of hyperexcitability.

ADK-Dependent Control of BDNF Signaling at Synapses

Our results also show that ADK levels not only affect tonic activation of the abundant A_1Rs in the hippocampus, but also tonic activation of A_{2A}R, which in spite of their modest direct synaptic influence and weak expression in the hippocampus (Sebastião and Ribeiro 1992; Cunha et al. 1994) have important modulatory roles. One such important regulatory role of the A_{2A}R in the hippocampus is the ability to gate BDNF/TrkB-mediated synaptic modulation (Sebastião et al. 2011). Remarkably, the facilitatory action of BDNF upon synaptic transmission is markedly influenced by age, and it has been proposed that this could be related to age-dependent changes in the degree of activation of adenosine receptors (Diógenes et al. 2004, 2007, 2011). By evaluating the effect of BDNF upon synaptic transmission in animals with different levels of expression of ADK as well as different ages, we found that variation in ADK expression abrogates the influence of age upon the A_{2A}R-dependent facilitatory action of BDNF on synaptic transmission: Young mice underexpressing ADK responded to BDNF to the same degree as adult mice with the same genotype. Conversely, the ability of BDNF to facilitate hippocampal synaptic transmission was completely lost in adult mice overexpressing ADK. In all cases, the effect of BDNF was lost upon A_{2A}R blockade. The influence of genotype over the BDNF effect upon synaptic transmission could not be attributed to changes in the levels of TrkB receptors (FL or truncated receptors) and AMPA (GluA1) or NMDA (GluN2B) receptor subunits. Together, these data demonstrate that ADK activity, by controlling extracellular levels of adenosine and the activation of A_{2A}R, crucially regulates the facilitatory action of BDNF at synapses.

ADK-Dependent Control of GABAergic Currents

Repeated activation of $GABA_A$ receptors results in the rundown of I_{GABA}. Such activity-dependent decrease in inhibitory currents promotes hyperexcitability of neurons. Indeed, exacerbated I_{GABA} rundown, together with a slow recovery, is a characteristic of epileptic tissue (Roseti et al. 2008). Here, we show that in CA1 pyramidal neurons (but not interneurons), the stability of I_{GABA} was influenced by ADK expression levels: Reducing ADK expression enhanced the activity-dependent I_{GABA} rundown, while overexpression of ADK significantly reduced the rundown of I_{GABA}. These observations suggest that extracellular adenosine facilitates I_{GABA} rundown upon repetitive stimulations. Indeed, the adenosine receptor antagonist CGS 15943 increased I_{GABA} stability, confirming the role of adenosine receptors in this phenomenon.

Whether the increased expression of ADK in seizure-induced astrogliosis retards the activity-dependent rundown of GABAergic currents remains to be determined, as does the observation that I_{GABA} in interneurons is not affected by the expression level of ADK and therefore by the extracellular levels of adenosine. Future studies are warranted to discern possible mechanisms underlying this cell specificity, which may involve differential adenosine receptor expression or a different local control of adenosine. Nonetheless, these data confirm the crucial role of the adenosinergic tone on modulating the stability of inhibitory transmission in hippocampal circuitry and open new paths for the study of local, adenosine receptor-mediated modulation of synaptic transmission, likely contributing to building effective therapeutic strategies for epilepsy.

ADK as an Upstream Regulator of Synaptic Networks

Although adenosine is a well-characterized endogenous anticonvulsant, suppressing seizures via the activation of A_1Rs (Boison and Stewart 2009), the role of neurotrophins in epilepsy is still a matter of debate. While BDNF can exacerbate epileptogenesis by promoting dysfunctional plasticity and circuit rewiring, it can also be protective against epilepsy-induced neuronal damage (Simonato et al. 2006; Paradiso et al. 2011). Since A_{2A}R gate synaptic actions of BDNF, adenosine, regulated by ADK, might affect epileptogenesis and ictogenesis through a BDNF-dependent pathway that is independent from the A_1R-dependent anticonvulsive effects of adenosine. The dual role of adenosine in epilepsy and activity-induced neuronal damage is further reflected by findings, indicating that A_{2A}R, by enhancing glutamate release, can exacerbate excitotoxicity (Marchi et al. 2002), whereas A_1Rs, by inhibiting glutamate release (Dolphin and Prestwich 1985) and NMDA receptor activation (de Mendonça et al. 1995), have neuroprotective actions against a wide range of neuronal insults (Sebastião et al. 2011). Pro- and anti-inflammatory actions of adenosine also occur (Ferrero 2011; Lopes et al. 2011) and should be taken into account whenever neuroprotective adenosine-based strategies are considered.

The identification of ADK as an upstream regulator of synaptic networks has pathophysiological implications that go beyond epilepsy. We recently demonstrated that adenosine dysregulation is implicated in the expression of schizophrenia-like symptoms in mice and that therapeutic adenosine augmentation might be of benefit for the psychotic and cognitive impairments in schizophrenia (Shen et al. 2012). Further, astrogliosis is a common pathological hallmark of many neurological conditions including epilepsy, Alzheimer's disease, and Parkinson's disease. Since overexpression of ADK has been associated with astrogliosis not only in several models of epilepsy (Gouder et al. 2004; Li, Ren et al. 2008; Aronica et al. 2011; Masino et al. 2011; de Groot et al. 2012), but also in samples from patients with Alzheimer's disease or amyotrophic lateral sclerosis (unpublished data). Those findings suggest that overexpression of ADK and associated adenosine deficiency is a common pathological trait across several neurological conditions, which share a variety of co-morbidities including cognitive impairment and sleep dysfunction. Thus, our present data suggest that any pathological disruption of adenosine homeostasis has far reaching consequences on complex network functions.

Therapeutic Implications

Overexpression of ADK through astrogliosis and resulting adenosine deficiency are pathological hallmarks of the epileptic brain (Li et al. 2007; Aronica et al. 2011; Masino et al. 2012). Consequently, adenosine augmentation therapies are considered as rational approaches for seizure suppression in epilepsy (Boison 2009; Boison and Stewart 2009). Adenosine augmentation strategies are not only thought to be of therapeutic value for the treatment of epilepsy but also for neuropsychiatric conditions, such as schizophrenia, where adenosine homeostasis might be affected (Boison et al. 2012). The therapeutic efficacy of adenosine augmentation therapies might be tightly linked to their ability to affect homeostatic control of network functions (Boison et al. 2011). Our present results suggest that conventional pharmacotherapeutic approaches to modulate adenosine receptor function with selective ligands is not likely a viable therapeutic option for the treatment of epilepsy and may suffer the same fate as conventional pharmacotherapeutic strategies, which fail in about 35% of all patients with epilepsy. Rather, the therapeutic reconstruction of functional adenosine homeostasis might provide a unique opportunity to capitalize on the multiple signaling pathways regulated by adenosine and might be achieved by pharmacological or genetic modulation of ADK activity.

Funding

The work done in Portugal was supported by Fundação para a Ciência e Tecnologia (FCT) and EU (COST B-30) concerted action. Work from the UK was supported by an Epilepsy Research UK PhD studentship to J.L. Work performed in the USA was supported by NIH grants R01-NS061844 and R01 NS065957. Work in Italy was supported by the Ministero della Salute, PRIN 2009.

Notes

We thank Regeneron for the gift of brain-derived neurotrophic factor, WW Andersen (University of Bristol, Bristol, UK) for the data analysis (LTP) program and Professor Nicholas Dale (University of Warwick) for valuable assistance in the use of biosensors. The animal housing facilities of the Institute of Physiology of the Faculty of Medicine of the University of Lisbon are also acknowledged. *Conflict of Interest*: B.G.F. is a Director of Sarissa Biomedical Ltd, the company from which the adenosine biosensors were purchased. J.L. has been an employee of Sarissa Biomedical Ltd.

References

Anderson WW, Collingridge GL. 2001. The LTP Program: A data acquisition program for on-line analysis of long-term potentiation and other synaptic events. J Neurosci Methods. 108:71–83.

Aronica E, Zurolo E, Iyer A, de Groot M, Anink J, Carbonell C, van Vliet EA, Baayen JC, Boison D, Gorter JA. 2011. Upregulation of adenosine kinase in astrocytes in experimental and human temporal lobe epilepsy. Epilepsia. 52:1645–1655.

Assaife-Lopes N, Sousa VC, Pereira DB, Ribeiro JA, Chao MV, Sebastião AM. 2010. Activation of adenosine A2A receptors induces TrkB translocation and increases BDNF-mediated phospho-TrkB localization in lipid rafts: Implications for neuromodulation. J Neurosci. 30:8468–8480.

Boison D. 2009. Adenosine augmentation therapies (AATs) for epilepsy: Prospect of cell and gene therapies. Epilepsy Res. 85:131–141.

Boison D, Chen JF, Fredholm BB. 2010. Adenosine signaling and function in glial cells. Cell Death Differ. 17:1071–1082.

Boison D, Masino SA, Geiger JD. 2011. Homeostatic bioenergetic network regulation—a novel concept to avoid pharmacoresistance in epilepsy. Expert Opin Drug Discov. 6:713–724.

Boison D, Singer P, Shen HY, Feldon J, Yee BK. 2012. Adenosine hypothesis of schizophrenia—opportunities for pharmacotherapy. Neuropharmacology. 62:1527–1543.

Boison D, Stewart KA. 2009. Therapeutic epilepsy research: From pharmacological rationale to focal adenosine augmentation. Biochem Pharmacol. 78:1428–1437.

Chitwood RA, Jaffe DB. 1998. Calcium-dependent spike-frequency accommodation in hippocampal CA3 nonpyramidal neurons. J Neurophysiol. 80:983–988.

Cunha RA, Johansson B, van der Ploeg I, Sebastião AM, Ribeiro JA, Fredholm BB. 1994. Evidence for functionally important adenosine A2a receptors in the rat hippocampus. Brain Res. 649:208–216.

de Groot M, Iyer A, Zurolo E, Anink J, Heimans JJ, Boison D, Reijneveld CJ, Aronica E. 2012. Overexpression of ADK in human astrocytic tumors and peritumoral tissue is related to tumor-associated epilepsy. Epilepsia. 53:58–66.

de Mendonça A, Sebastião AM, Ribeiro JA. 1995. Inhibition of NMDA receptor-mediated currents in isolated rat hippocampal neurones by adenosine A1 receptor activation. Neuroreport. 6:1097–1100.

Diógenes MJ, Assaife-Lopes N, Pinto-Duarte A, Ribeiro JA, Sebastião AM. 2007. Influence of age on BDNF modulation of hippocampal synaptic transmission: Interplay with adenosine A2A receptors. Hippocampus. 17:577–585.

Diógenes MJ, Costenla AR, Lopes LV, Jerónimo-Santos A, Sousa VC, Fontinha BM, Ribeiro JA, Sebastião AM. 2011. Enhancement of LTP in aged rats is dependent on endogenous BDNF. Neuropsychopharmacology. 36:1823–1836.

Diógenes MJ, Fernandes CC, Sebastião AM, Ribeiro JA. 2004. Activation of adenosine A2A receptor facilitates brain-derived neurotrophic factor modulation of synaptic transmission in hippocampal slices. J Neurosci. 24:2905–2913.

Dolphin AC, Prestwich SA. 1985. Pertussis toxin reverses adenosine inhibition of neuronal glutamate release. Nature. 316:148–150.

Dunwiddie TV. 1980. Endogenously released adenosine regulates excitability in the in vitro hippocampus. Epilepsia. 21:541–548.

Etherington LA, Frenguelli BG. 2004. Endogenous adenosine modulates epileptiform activity in rat hippocampus in a receptor subtype-dependent manner. Eur J Neurosci. 19:2539–2550.

Etherington LA, Patterson GE, Meechan L, Boison D, Irving AJ, Dale N, Frenguelli BG. 2009. Astrocytic adenosine kinase regulates basal synaptic adenosine levels and seizure activity but not activity-dependent adenosine release in the hippocampus. Neuropharmacology. 56:429–437.

Fedele DE, Gouder N, Guttinger M, Gabernet L, Scheurer L, Rulicke T, Crestani F, Boison D. 2005. Astrogliosis in epilepsy leads to overexpression of adenosine kinase, resulting in seizure aggravation. Brain. 128:2383–2395.

Fernandes CC, Pinto-Duarte A, Ribeiro JA, Sebastião AM. 2008. Postsynaptic action of brain-derived neurotrophic factor attenuates alpha7 nicotinic acetylcholine receptor-mediated responses in hippocampal interneurons. J Neurosci. 28:5611–5618.

Ferrero ME. 2011. Purinoceptors in inflammation: Potential as anti-inflammatory therapeutic targets. Front Biosci. 17:2172–2186.

Fontinha BM, Diógenes MJ, Ribeiro JA, Sebastião AM. 2008. Enhancement of long-term potentiation by brain-derived neurotrophic factor requires adenosine A2A receptor activation by endogenous adenosine. Neuropharmacology. 54:924–933.

Frenguelli BG, Llaudet E, Dale N. 2003. High-resolution real-time recording with microelectrode biosensors reveals novel aspects of adenosine release during hypoxia in rat hippocampal slices. J Neurochem. 86:1506–1515.

Frenguelli BG, Wigmore G, Llaudet E, Dale N. 2007. Temporal and mechanistic dissociation of ATP and adenosine release during

ischaemia in the mammalian hippocampus. J Neurochem. 101:1400–1413.
Gouder N, Scheurer L, Fritschy J-M, Boison D. 2004. Overexpression of adenosine kinase in epileptic hippocampus contributes to epileptogenesis. J Neurosci. 24:692–701.
Kamiya H, Shinozaki H, Yamamoto C. 1996. Activation of metabotropic glutamate receptor type 2/3 suppresses transmission at rat hippocampal mossy fibre synapses. J Physiol. 493(Pt 2):447–455.
Kukley M, Schwan M, Fredholm BB, Dietrich D. 2005. The role of extracellular adenosine in regulating mossy fiber synaptic plasticity. J Neurosci. 25:2832–2837.
Lacaille JC, Mueller AL, Kunkel DD, Schwartzkroin PA. 1987. Local circuit interactions between oriens/alveus interneurons and CA1 pyramidal cells in hippocampal slices: Electrophysiology and morphology. J Neurosci. 7:1979–1993.
Li T, Lan JQ, Boison D. 2008. Uncoupling of astrogliosis from epileptogenesis in adenosine kinase (ADK) transgenic mice? Neuron Glia Biol. 4:91–99.
Li T, Quan Lan J, Fredholm BB, Simon RP, Boison D. 2007. Adenosine dysfunction in astrogliosis: Cause for seizure generation. Neuron Glia Biol. 3:353–366.
Li T, Ren G, Lusardi T, Wilz A, Lan JQ, Iwasato T, Itohara S, Simon RP, Boison D. 2008. Adenosine kinase is a target for the prediction and prevention of epileptogenesis in mice. J Clin Invest. 118:571–582.
Lopatar J, Dale N, Frenguelli BG. 2011. Minor contribution of ATP P2 receptors to electrically-evoked electrographic seizure activity in hippocampal slices: Evidence from purine biosensors and P2 receptor agonists and antagonists. Neuropharmacology. 61:25–34.
Lopes LV, Sebastião AM, Ribeiro JA. 2011. Adenosine and related drugs in brain diseases: Present and future in clinical trials. Curr Top Med Chem. 11:1087–1101.
Lovatt D, Xu Q, Liu W, Takano T, Smith NA, Schnermann J, Tieu K, Nedergaard M. 2012. Neuronal adenosine release, and not astrocytic ATP release, mediates feedback inhibition of excitatory activity. Proc Natl Acad Sci USA. 109:6265–6270.
Marchi M, Raiteri L, Risso F, Vallarino A, Bonfanti A, Monopoli A, Ongini E, Raiteri M. 2002. Effects of adenosine A1 and A2A receptor activation on the evoked release of glutamate from rat cerebrocortical synaptosomes. Br J Pharmacol. 136:434–440.
Masino SA, Kawamura M Jr, Ruskin DN, Geiger JD, Boison D. 2012. Purines and neuronal excitability: Links to the ketogenic diet. Epilepsy Res. 100:229–238
Masino SA, Li T, Theofilas P, Sandau US, Ruskin DN, Fredholm BB, Geiger JD, Aronica E, Boison D. 2011. A ketogenic diet suppresses seizures in mice through adenosine A1 receptors. J Clin Inv. 121:2679–2683.
Moore KA, Nicoll RA, Schmitz D. 2003. Adenosine gates synaptic plasticity at hippocampal mossy fiber synapses. Proc Natl Acad Sci USA. 100:14397–14402.
Paradiso B, Zucchini S, Su T, Bovolenta R, Berto E, Marconi P, Marzola A, Navarro Mora G, Fabene PF, Simonato M. 2011. Localized overexpression of FGF-2 and BDNF in hippocampus reduces mossy fiber sprouting and spontaneous seizures up to 4 weeks after pilocarpine-induced status epilepticus. Epilepsia. 52:572–578.
Pignataro G, Maysami S, Studer FE, Wilz A, Simon RP, Boison D. 2008. Downregulation of hippocampal adenosine kinase after focal ischemia as potential endogenous neuroprotective mechanism. J Cereb Blood Flow Metab. 28:17–23.
Pignataro G, Simon RP, Boison D. 2007. Transgenic overexpression of adenosine kinase aggravates cell death in ischemia. J Cereb Blood Flow Metab. 27:1–5.
Pousinha PA, Diógenes MJ, Ribeiro JA, Sebastião AM. 2006. Triggering of BDNF facilitatory action on neuromuscular transmission by adenosine A2A receptors. Neurosci Lett. 404:143–147.
Ragozzino D, Palma E, Di Angelantonio S, Amici M, Mascia A, Arcella A, Giangaspero F, Cantore G, Di Gennaro G, Manfredi M *et al*. 2005. Rundown of GABA type A receptors is a dysfunction associated with human drug-resistant mesial temporal lobe epilepsy. Proc Natl Acad Sci USA. 102:15219–15223.
Rex CS, Kramar EA, Colgin LL, Lin B, Gall CM, Lynch G. 2005. Long-term potentiation is impaired in middle-aged rats: Regional specificity and reversal by adenosine receptor antagonists. J Neurosci. 25:5956–5966.
Roseti C, Martinello K, Fucile S, Piccari V, Mascia A, Di Gennaro G, Quarato PP, Manfredi M, Esposito V, Cantore G *et al*.. 2008. Adenosine receptor antagonists alter the stability of human epileptic GABAA receptors. Proc Natl Acad Sci USA. 105:15118–15123.
Roseti C, Palma E, Martinello K, Fucile S, Morace R, Esposito V, Cantore G, Arcella A, Giangaspero F, Aronica E *et al*.. 2009. Blockage of A2A and A3 adenosine receptors decreases the desensitization of human GABA(A) receptors microtransplanted to *Xenopus* oocytes. Proc Natl Acad Sci USA. 106:15927–15931.
Sebastião AM. 2010. Adenosine and epilepsy—thinking beyond A(1) receptors. Purinergic Signal. 6:1–2.
Sebastião AM, Assaife-Lopes N, Diógenes MJ, Vaz SH, Ribeiro JA. 2011. Modulation of brain-derived neurotrophic factor (BDNF) actions in the nervous system by adenosine A(2A) receptors and the role of lipid rafts. Biochim Biophys Acta. 1808:1340–1349.
Sebastião AM, Ribeiro JA. 1992. Evidence for the presence of excitatory A2 adenosine receptors in the rat hippocampus. Neurosci Lett. 138:41–44.
Sebastião AM, Ribeiro JA. 2009. Tuning and fine-tuning of synapses with adenosine. Curr Neuropharmacol. 7:180–194.
Sebastião AM, Stone TW, Ribeiro JA. 1990. The inhibitory adenosine receptor at the neuromuscular junction and hippocampus of the rat: Antagonism by 1,3,8-substituted xanthines. Br J Pharmacol. 101:453–459.
Shen HY, Lusardi TA, Williams-Karnesky RL, Lan JQ, Poulsen DJ, Boison D. 2011. Adenosine kinase determines the degree of brain injury after ischemic stroke in mice. J Cereb Blood Flow Metab. 31:1648–1659.
Shen HY, Singer P, Lytle N, Wei CJ, Lan JQ, Williams-Karnesky RL, Chen JF, Yee BK, Boison D. 2012. Adenosine augmentation ameliorates psychotic and cognitive endophenotypes of schizophrenia. J Clin Invest. 122:2567–2577.
Simonato M, Tongiorgi E, Kokaia M. 2006. Angels and demons: Neurotrophic factors and epilepsy. Trends Pharmacol Sci. 27:631–638.
Studer FE, Fedele DE, Marowsky A, Schwerdel C, Wernli K, Vogt K, Fritschy JM, Boison D. 2006. Shift of adenosine kinase expression from neurons to astrocytes during postnatal development suggests dual functionality of the enzyme. Neuroscience. 142: 125–137.
Tebano MT, Martire A, Potenza RL, Gro C, Pepponi R, Armida M, Domenici MR, Schwarzschild MA, Chen JF, Popoli P. 2008. Adenosine A(2A) receptors are required for normal BDNF levels and BDNF-induced potentiation of synaptic transmission in the mouse hippocampus. J Neurochem. 104:279–286.
Wilz A, Pritchard EM, Li T, Lan JQ, Kaplan DL, Boison D. 2008. Silk polymer-based adenosine release: Therapeutic potential for epilepsy. Biomaterials. 29:3609–3616.
Yee BK, Singer P, Chen JF, Feldon J, Boison D. 2007. Transgenic overexpression of adenosine kinase in brain leads to multiple learning impairments and altered sensitivity to psychomimetic drugs. Eur J Neurosci. 26:3237–3252.
zur Nedden S, Hawley S, Pentland N, Hardie DG, Doney AS, Frenguelli BG. 2011. Intracellular ATP influences synaptic plasticity in area CA1 of rat hippocampus via metabolism to adenosine and activity-dependent activation of adenosine A1 receptors. J Neurosci. 31:6221–6234.